Neurobiology of Disease 74 (2015) 325–335

Contents lists available at ScienceDirect

Neurobiology of Disease

journal homepage: www.elsevier.com/locate/ynbdi

Prolonged treatment with pramipexole promotes physical interaction of striatal dopamine D3 autoreceptors with dopamine transporters to reduce dopamine uptake

Javier Castro-Hernández [a], Domingo Afonso-Oramas [a], Ignacio Cruz-Muros [a], Josmar Salas-Hernández [a], Pedro Barroso-Chinea [a], Rosario Moratalla [b,d], Mark J. Millan [c], Tomás González-Hernández [a,d,*]

[a] Departamento de Anatomía, Facultad de Medicina, Instituto de Tecnologías Biomédicas (ITB, CIBICAN), Universidad de La Laguna, Tenerife, Spain
[b] Departamento de Biología Funcional y de Sistemas, Instituto Cajal, Consejo Superior de Investigaciones Científicas, Madrid, Spain
[c] Pole of Innovation in Neuropsychopharmacology, Institut de Recherches Servier, 78290 Croissy sur Seine, France
[d] Centro de investigación Biomédica en Red sobre enfermedades neurodegenerativas, CIBERNED, Instituto de Salud Carlos III, Spain

ARTICLE INFO

Article history:
Received 1 September 2014
Revised 14 November 2014
Accepted 5 December 2014
Available online 12 December 2014

Keywords:
Dopamine transporter
D_3R
D_2R
Dopamine autoreceptor
Multi-protein complex
Neuroprotection
Parkinson's disease
Depression

ABSTRACT

The dopamine (DA) transporter (DAT), a membrane glycoprotein expressed in dopaminergic neurons, clears DA from extracellular space and is regulated by diverse presynaptic proteins like protein kinases, α-synuclein, D_2 and D_3 autoreceptors. DAT dysfunction is implicated in Parkinson's disease and depression, which are therapeutically treated by dopaminergic D_2/D_3 receptor (D_2/D_3R) agonists. It is, then, important to improve our understanding of interactions between D_3R and DAT. We show that prolonged administration of pramipexole (0.1 mg/kg/day, 6 to 21 days), a preferential D_3R agonist, leads to a decrease in DA uptake in mouse striatum that reflects a reduction in DAT affinity for DA in the absence of any change in DAT density or subcellular distribution. The effect of pramipexole was absent in mice with genetically-deleted D_3R ($D_3R^{-/-}$), yet unaffected in mice genetically deprived of D_2R ($D_2R^{-/-}$). Pramipexole treatment induced a physical interaction between D_3R and DAT, as assessed by co-immunoprecipitation and in situ proximity ligation assay. Furthermore, it promoted the formation of DAT dimers and DAT association with both D_2R and α-synuclein, effects that were abolished in $D_3R^{-/-}$ mice, yet unaffected in $D_2R^{-/-}$ mice, indicating dependence upon D_3R. Collectively, these data suggest that prolonged treatment with dopaminergic D_3 agonists provokes a reduction in DA reuptake by dopaminergic neurons related to a hitherto-unsuspected modification of the DAT interactome. These observations provide novel insights into the *long-term* antiparkinson, antidepressant and additional clinical actions of pramipexole and other D_3R agonists.

Introduction

Dopamine (DA) is a major neurotransmitter exerting actions on locomotor activity, motivation, reward, and cognition. The intensity and duration of DA signaling are regulated by the dopamine transporter (DAT), a membrane protein expressed in dopaminergic (DA-) cells, which is responsible for the reuptake of extracellular DA into presynaptic terminals (Mortensen and Amara, 2003). DAT dysfunction is involved in neurological and psychiatric conditions, such as Parkinson's disease, attention deficit hyperactivity disorder, schizophrenia, bipolar disorder and psychostimulant abuse (Afonso-Oramas et al., 2009; Amsterdam et al., 2012; Bowton et al., 2010).

DAT activity is under the control of different presynaptic proteins, including DA D_2 and D_3 autoreceptors, that promote either trafficking and availability of the transporter at the plasma membrane (Mortensen and Amara, 2003; Torres, 2006), or its internalization for it to be either degraded or recycled back to the plasma membrane (Ericksen et al., 2010; Miranda and Sorkin, 2007). The effects of the D_2 autoreceptor on DAT are relatively well known. Current data suggest that it induces recruitment of DAT to the plasma membrane and likewise facilitates DA uptake (Bolan et al., 2007; Lee et al., 2007). This effect probably involves both physical coupling between DAT and D_2 receptor (D_2R) independently of the presence of ligands (Lee et al., 2007), and activation of the PKCβ-ERK1/2 signaling cascade through D_2R stimulation (Bolan et al., 2007; Chen et al., 2013).

Conversely, knowledge about the influence of D_3 receptor (D_3R) on DAT is still fragmentary. On the one hand, this reflects the comparatively modest density of D_3 autoreceptors (Diaz et al., 2000; Sokoloff et al., 1990) and, on the other hand, the limited selectivity of agonists for D_3R (Millan, 2010; Wang et al., 2010), making it difficult to distinguish D_3R from D_2R actions. Moreover, the existence of D_2R-D_3R heteromers complicates the task of identifying the precise significance of D_3R (and D_2R) (Maggio and Millan, 2010). Studies of the impact of D_3R

* Corresponding author at: Department of Anatomy, Faculty of Medicine, University of La Laguna, 38207 La Laguna, Tenerife, Spain. Fax: +34 922 660253.
E-mail address: tgonhern@ull.es (T. González-Hernández).
Available online on ScienceDirect (www.sciencedirect.com).

http://dx.doi.org/10.1016/j.nbd.2014.12.007
0969-9961/

autoreceptors on DAT functional activity have mostly focussed on the effects of acute D_3R stimulation, which increases DAT activity (Zapata et al., 2007; Zapata and Shippenberg, 2005). In contrast, a study of subchronic treatment with the D_3R preferential agonist pramipexole (PPX) in mice reported a decrease in DAT activity (Joyce et al., 2004), suggesting the occurrence of adaptive events.

Inasmuch as PPX and other D_3R preferential agonists are widely used in the treatment of Parkinson's disease (Albrecht and Buerger, 2009; Millan, 2010; Parkinson Study Group CALM cohort investigators, 2009), and D_3Rs are potentially important targets for the control of psychiatric disorders involving DAT dysfunction (Amsterdam et al., 2012; Sokoloff et al., 2006), there is a need for better knowledge about D_3R–DAT interactions, and particularly the effects of long-term administration of D_3R agonists. In order to address this issue, we analyzed the effects of a prolonged treatment of mice with PPX on DAT association with protein partners and DA uptake in the mouse striatum, a structure innervated by substantia nigra DA neurons and enriched in DAT (Afonso-Oramas et al., 2009). Furthermore, in order to confirm the potential significance of D_3R to the actions of PPX, studies were undertaken in mice genetically deprived of D_3R ($D_3R^{-/-}$, Accili et al., 1996; Collo et al., 2012) as compared to mice with genetically deleted D_2R ($D_2R^{-/-}$, Granado et al., 2011; Kelly et al., 1997). Taken together, the results suggest that chronic exposure to PPX decreases the affinity of DAT (for DA) in parallel with changes in its interactions with D_3 autoreceptors and other protein partners.

Material and methods

Animals and treatment

The experiments were carried out on 22–24 g (4–6 months old) male C57BL/6J mice, DA D_3 receptor knockout ($D_3R^{-/-}$), and $D_2R^{-/-}$ mice and their wild-type (WT) littermates . $D_3R^{-/-}$ were obtained from the Jackson Laboratory (B6.129S4-Drd3Tm1Dac/J) (Accili et al., 1996; Collo et al., 2012). Homozygous $D_3R^{-/-}$ mice were generated on a pure genetic background (C57BL/6J). The $D_2R^{-/-}$ mice were generated by homologous recombination as previously described (Kelly et al., 1997). D_2 $R^{-/-}$ and their WT littermates were obtained by mating heterozygous mice (Granado et al., 2011). Genotype was determined by polymerase chain reaction. Mice were housed in groups of 3–4 per cage, in conditions of constant temperature (21–22 °C), a 12 h light/dark cycle, and given free access to food and water. Experimental protocols were approved by the Ethical Committee of the University of La Laguna (Reference # 091/010), and are in accordance with the European Communities Council Directive of 22 September 2010 (2010/63/EU) regarding the care and use of animals for scientific purposes.

Mice were treated for six days with a single daily dose of PPX (pramipexole dihydrochloride, Sigma, St. Louis, MO) or its vehicle (50 μl 0.9% sterile saline i.p.) and killed on day seven. We choose PPX because it is a DA D_3R preferential agonist extensively used for the treatment of Parkinson's disease. According to Piercey et al. (1996), PPX Ki is 0.9, 6.9 and 15 nM for D_3R, D_2R and D_4R respectively, indicating that its affinity for D_3R is 7 times higher than for D_2R and 17 times higher than for D_4R. Doses ranging between 0.05 and 1.5 mg/kg/day were checked by [^{3}H]-DA uptake in striatal synaptosomes to establish the lowest dose which, under this administration schedule, has bioactive effects on DAT. Preliminary experiments showed a significant DA uptake decrease from 0.1 mg/kg (Fig. 1A), so this dose was used in all experiments. This treatment was maintained for 21 days in some C57BL/6J mice. In two groups of C57BL/6J mice, the selective D_2R antagonist L741,626 (1 mg/kg, s.c.; Sigma) or the selective D_3R antagonist NGB2904 (1 mg/kg, i.p.; R & D Systems, Minneapolis, MN), or their vehicle (0.05% lactic acid, s.c., or 25% w/v 2-hydroxypropyl-β-cyclodextrin, i.p., respectively; 50 μl) was injected 30 min before PPX. The drug doses and injection time before PPX used here were shown by others to have D_2 or D_3 antagonist specific effects (Collins et al., 2007; Joyce et al., 2004; Kofarnus et al., 2009; Mason et al., 2010; Millan et al., 2000). Experimental groups included at least 5 mice in each experiment.

Synaptosomal [^{3}H]-DA uptake

This procedure was performed according to Afonso-Oramas et al. (2009). The mouse striata were dissected in ice from freshly obtained brains using a brain blocker. Samples were immediately homogenized in 20 vol of ice-cold sucrose bicarbonate solution (SBS, 320 mM sucrose in 5 mM sodium bicarbonate, pH 7.4) with 12 up and down strokes in a Teflon-glass homogenizer. The homogenates were centrifuged (1000 ×*g*, 10 min, 4 °C), and the pellets (P1) containing nuclei and large debris discarded. The supernatants (S1) were centrifuged (17,000 ×*g*, 20 min, 4 °C), and the pellets (P2) were resuspended in 500 μl ice-cold assay buffer (125 mM NaCl, 5 mM KCl, 1.5 mM $MgSO_4$, 1.25 mM $CaCl_2$, 1.5 mM KH_2PO_2, 10 mM glucose, 25 mM HEPES, 0.1 mM EDTA, 0.1 mM pargyline and 0.1 mM ascorbic acid). For [^{3}H]-DA uptake assays, a range of temperatures (25–35 °C), DA concentrations (20–500 nM), incubation times (5–30 min) and striatal protein concentrations (0.2–3 μg/μl) were checked in order to establish the working parameters in the linear ascending segment of the uptake curve. Fifty microliters of synaptosomal suspension (0.5 μg total protein/μl) was preincubated with 50–500 nM DA (Sigma; with or without 10 μM nomifensine, Sigma) in assay buffer (30 °C, 5 min). Subsequently, 20 nM [^{3}H]-DA (final concentration; Amersham, Buckinghamshire, UK) was added to each tube. The total assay volume was 200 μl. After a 10 min incubation at 30 °C, DA uptake was stopped by the addition of 200 μl ice-cold assay buffer. The suspension was immediately filtered under vacuum through MultiScreen®-0.45 μm hydrophilic filters (Millipore, Molsheim, France). The filters were washed twice with 200 μl ice-cold assay buffer, excised and placed in scintillation vials containing 3 ml liquid scintillation Cocktail (Sigma), and stored overnight at room temperature (RT). Accumulated radioactivity was quantified using a liquid scintillation counter (LKB Rackbeta 1214; Turku, Finland). Non-specific uptake, defined as the DA uptake in the presence of nomifensine, was subtracted from total uptake to define DAT-mediated specific uptake. All assays were performed in triplicate. V_{max} and K_m values were determined by non-linear regression.

DAT antibodies

Several commercial anti-DAT antibodies against different fragments of human and rat DAT have been tested in our laboratory. Brain samples of different mammals, including humans and mice, and cells transfected with wild type and mutated DAT forms, were subjected to immunohistochemistry, western-blot and immunoprecipitation (see Afonso-Oramas et al., 2009, 2010; Cruz-Muros et al., 2009). These experiments were used to determine their specificity and sensitivity, as well as which band (glycosylated, 75 kDa; partially glycosylated, 68 kDa, and non-glycosylated, 50 kDa) is detected by each of them (Afonso-Oramas et al., 2009). Taking these tests into account, it was decided to use a goat anti-DAT polyclonal antibody (Santa Cruz Biotechnology, Santa Cruz, CA) for immunohistochemistry, western-blot and in situ proximity ligation assays, and a rabbit anti-DAT polyclonal antibody (Millipore, Billerica, MA) for immunoprecipitation and in situ proximity ligation assays, both of which recognize the glycosylated (75 kDa) DAT form.

DAT immunohistochemistry

Mice were deeply anesthetized with an overdose of sodium pentobarbital and transcardially perfused with heparinized ice-cold 0.9% saline (20 ml) followed by 4% paraformaldehyde in phosphate buffered saline pH 7.4 (PBS, 50 ml). The brains were removed and stored overnight in the same fixative at 4 °C, cryoprotected in a graded series of

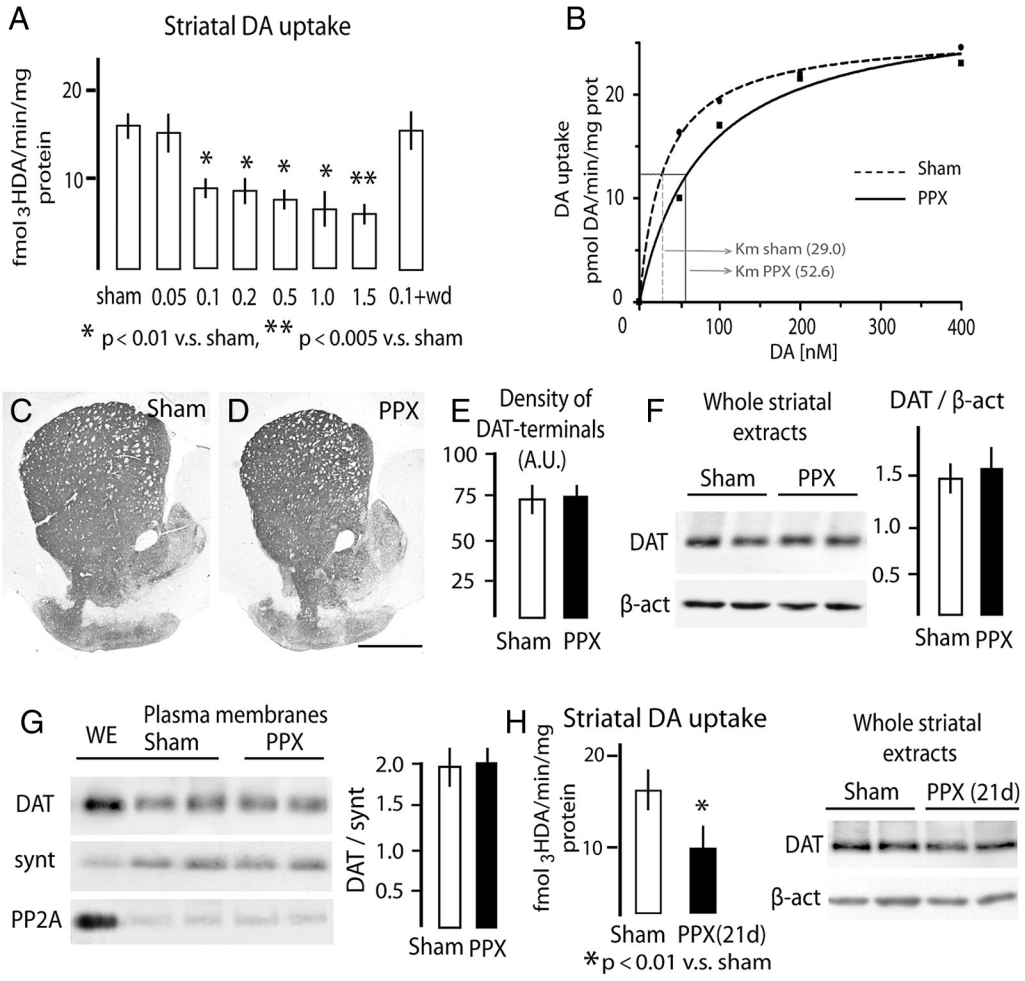

Fig. 1. DA uptake and DAT expression in the C57BL/6J mouse striatum after treatment with the dopamine D_3 receptor preferential agonist pramipexole (PPX). (A) Mice were treated with different doses of PPX (0.05–1.5 mg/kg/day) for six days. Striatal DA uptake was significantly lower in mice receiving ≥0.1 mg/kg/day. DA uptake returned to normal levels after 5 days of treatment withdrawal (0.1 + wd). (B) Kinetics analysis showed that the DA uptake decrease coincides with an increase in K_m (decrease in DAT affinity) and no changes in V_{max}. (C–E) Immunohistochemistry for DAT revealed no immunostaining differences between the striatum of sham and PPX-treated mice. (F, G) Western-blot of whole striatal extracts (F) and the plasma membrane of striatal synaptosomes (G) also showed no differences in DAT expression levels between treated and untreated mice. (H) DA uptake and DAT expression in the striatum after 21 days of treatment with PPX (21 day; 0.1 mg/kg/day). Striatal DA uptake was significantly lower after treatment but DAT expression was unchanged. β-act, β-actin; PP2A, protein phosphatase 2A; synt, syntaxin; WE, whole extract; Bar in D (for C and D) 400 μm.

sucrose-PBS solutions and stored at −80 °C until processing. Coronal sections (25 μm) were obtained with a freezing microtome, collected in 6–8 parallel series and processed for DAT immunohistochemistry (Afonso-Oramas et al., 2009; Granado et al., 2011). Floating sections were immersed for 30 min in 3% H_2O_2 to inactivate endogenous peroxidase, and incubated for 60 min at RT in 4% normal donkey serum (NDS, Jackson ImmunoResearch, West Grove, PA) in PBS, containing 0.05% Triton X-100 (TX-100, Sigma), and left overnight in PBS containing 2% NDS and goat anti-DAT polyclonal antibody (Santa Cruz Biotechnology, 1: 400). After several rinses, the sections were incubated for 2 h in biotinylated donkey anti-goat antiserum (1:1000, Jackson ImmunoResearch) and 1:200 NDS in PBS. Immunoreactions were visible after incubation for 1 h at RT in ExtrAvidin-peroxidase (1:5000, Sigma) in PBS, and after 10 min in 0.005% 3′-3′-diamiobenzidine tetrahydrochloride (DAB, Sigma) and 0.001% H_2O_2 in cacodylate buffer 0.05 N pH 7.6.

The labeling intensity of striatal terminals was quantified following the densitometry procedure previously described (Gonzalez-Hernandez et al., 2004). Square areas of 100 μm × 100 μm were randomly selected in the dorsal striatum (10 areas per section, 6 sections 75 μm away from each other, and 5 mice per group). The labeling intensity of each area was compared with that of the neighboring corpus callosum. In order to prevent differences due to variations in protocol conditions during tissue processing and densitometric analysis, all sections were simultaneously processed using the same protocol and chemical reagents, and all microscopic and computer parameters were kept constant throughout the densitometric study. Microscopic images were digitalized and the labeling intensity was analyzed using densitometry software (Leica Microsystems, Wetzlar, Germany). The intensity of labeling was defined as the index of light attenuation with respect to the neighboring background and expressed as arbitrary units (A.U, range 0–256).

Western-blot in whole striatal extracts and plasma membranes

DAT expression was also studied using western-blot analysis of total extracts and the plasma membrane fraction of striatal synaptosomes. The striata were dissected as described for DA uptake. Whole protein extracts were obtained using the acid phenol method, resuspended in radioimmunoprecipitation assay (RIPA) lysis buffer pH 7.4, and quantified using the bicinchoninic acid method and bovine serum albumin as standard. Plasma membranes were obtained following the impermeant biotinylation procedure (Salvatore et al., 2003). Synaptosomes (300 μg total protein) were incubated for 1 h at 4 °C with continual shaking in 500 μl of 1.5 mg/ml sulfo-NHS-biotin (Pierce, Rockford, IL) in PBS/Ca/Mg buffer (138 mM Na Cl, 2.7 mM KCl, 1.5 mM KH_2PO_2,

9.6 mM Na_2HPO_4, 1 mM $MgCl_2$, 0.1 mM $CaCl_2$, pH 7.3) and centrifuged (8000 ×*g*, 4 min, 4 °C). In order to remove biotinylating reagents, the resulting pellets were resuspended in 1 ml ice-cold 100 mM glycine in PBS/Ca/Mg buffer and centrifuged (8000 ×*g*, 4 min, 4 °C). The resuspension and centrifugation steps were repeated. Final pellets were resuspended again in 1 ml ice-cold 100 mM glycine in PBS/Ca/Mg buffer and incubated for 30 min at 4 °C. Samples were washed three more times in PBS/Ca/Mg buffer, and then lysed by sonication for 2–4 s in 300 μl Triton X-100 buffer (10 mM Tris, pH 7.4, 150 mM NaCl, 1 mM EDTA, 1% Triton X-100) containing protease inhibitors (1 μg/ml aprotinin, 1 μg/ml leupeptin, 1 mM pepstatin, 250 μM phenylmethylsulfonyl fluoride). After incubation in continuous shaking (30 min, 4 °C), the lysates were centrifuged (18,000 ×*g*, 30 min, 4 °C), and the supernatants were incubated with monomeric avidin bead–Triton X-100 buffer (100 μl) for 1 h at RT, and centrifuged (18,000 ×*g*, 4 min, 4 °C). The resulting pellets (containing avidin-absorbed biotinylated surface proteins) were resuspended in 1 ml Triton X-100 buffer and centrifuged (18,000 ×*g*, 4 min, 4 °C). Resuspension and centrifugation were repeated two more times, and the final pellets were then stored.

Protein samples for western-blot analysis were diluted in Laemmli's loading buffer (62.5 mM Tris–HCl, 20% glycerol, 2% sodium dodecyl sulfate [SDS], 1.7% β-mercaptoethanol and 0.05% bromophenol blue, pH 6.8), denatured (90 °C, 1 min.), separated by electrophoresis in 10% SDS-polyacrylamide gel, and transferred to nitrocellulose (Schleicher & Schuell, Dassel, Germany). Blots were blocked for 2 h at RT with 5% non-fat dry milk in TBST (250 mM NaCl, 50 mM Tris, pH 7.4, and 0.05% Tween20), and incubated overnight at 4 °C in blocking solution with goat polyclonal anti-DAT antibody (Santa Cruz Biotechnology, 1:500). After several rinses in TBST-5% milk, the membranes were incubated for 1 h in horseradish peroxidase conjugated anti-goat IgG (Jackson-ImmunoResearch, West Grove, PA; 1:5000). Immunoreactive bands were visualized using enhanced chemiluminescence (Immun-Star, Bio-Rad, CA) and a Versa-Doc gel documentation system (Bio-Rad). Different protein quantities, antibody dilutions and exposure times were tested to establish the working range of each antibody. After DAT processing, each nitrocellulose membrane was subjected to stripping treatment (62.5 mM Tris, pH 6.8, 2% SDS, 100 mM β-mercaptoethanol; 1 h at RT), and processed for β-Actin using a mouse anti-β-Actin antibody (Sigma; 1:10,000, 2 h at RT). The labeling densities for DAT were compared with those of β-Actin by using densitometry software (Bio-Rad). A rectangle of uniform size and shape was placed over each band, and the density values were calculated by subtracting the background at approximately 2 mm above each band. The effectiveness of the plasma membrane fractionation was evaluated using Syntaxin (mouse monoclonal anti-syntaxin, 1:500; Sigma) as a marker of synaptosomal membrane, and PP2A (protein phosphatase 2A, rabbit polyclonal anti-PP2A, 1: 200; Santa Cruz Biotechnology) as a marker of synaptosomal cytosol.

Western-blot analysis under non-reducing conditions

Western-blot analysis under non-reducing conditions was performed according to Baucum et al. (2004). Briefly, synaptosomes were obtained as described for DA uptake using 0.32 M sucrose supplemented with protease inhibitor cocktail and 10 mM N-ethylmaleimide (NEM) as homogenization solution. P2 pellets were resuspended in milli-Q water, protein concentration was quantified, and the samples were mixed with loading buffer (2.25% SDS, 18% glycerol, 180 mM Tris base, pH 6.8, and bromophenol blue). Forty micrograms of total protein was loaded into each well, separated by electrophoresis in 9% SDS-polyacrylamide gel containing 0.1% SDS, and transferred to nitrocellulose (Schleicher & Schuell). DAT immunostaining and quantification were performed as described above.

Co-immunoprecipitation

Co-immunoprecipitation was performed according to Hadlock et al. (2011) with minor modifications. The striata of two mice were pooled and processed as a single sample for these experiments. Tissue was homogenized in 1.5 ml ice-cold 10 mM HEPES, 0.32 M sucrose and 10 mM NEM pH 7.4, and centrifuged (800 ×*g*, 12 min, 4 °C). The supernatants (S1) were centrifuged at 22,000 ×*g*, 15 min, 4 °C, and the resulting pellets (P2) resuspended in 100 μl M-PER (Thermo Scientific). After 1 h at 4 °C in gentle shaking, the samples were centrifuged again, the pellets were discarded, and the protein concentration was quantified in supernatants. Aliquots of 500 μg proteins were incubated in protein A-Sepharose beads (100 μl stock suspension in 200 μl M-PER; 4 °C, 45 min) to pre-clear endogenous immunoglobulins. After gentle centrifugation, pre-cleared supernatants were incubated with anti-DAT, anti-D_2R, anti-D_3R antibody or non-immune IgG overnight at 4 °C in continuous shaking. In the experience of this laboratory, the most robust immunoprecipitates are obtained using 6 μl of rabbit polyclonal anti-DAT from Millipore®, rabbit polyclonal anti-D_2R from Millipore® and mouse monoclonal anti-D_3R from Invitrogen®. Protein A-Sepharose beads (100 μl stock suspension in 200 μl M-PER) were added and maintained in continuous shaking at 4 °C for 3 h. Immunocomplexes were precipitated by gentle centrifugation. After extensive washing, they were resuspended in 40 μl Laemmli's buffer, denatured, separated by electrophoresis in 10% SDS-polyacrylamide gel and transferred to nitrocellulose. Blots from DAT precipitates were immunoreacted for α-synuclein and DAT using a mouse monoclonal anti-α-synuclein (1: 500, BD Biosciences, San Jose, CA) and a goat polyclonal anti-DAT antibody (1:500, Santa Cruz Biotechnology). Blots from D_2R precipitates were immunoreacted for DAT and D_2R using a goat anti-DAT polyclonal (1:500, Santa Cruz Biotechnology) and a mouse monoclonal anti-D_2R antibody (1:500, Santa Cruz Biotechnology). Blots from D_3R precipitates were immunoreacted for DAT and D_3R using a goat polyclonal anti-DAT (1:500, Santa Cruz Biotechnology) and a rabbit polyclonal anti-D_3R antibody (1: 300, Alomone labs, Jerusalem, Israel). Control experiments were performed in $D_2R^{-/-}$ and $D_3R^{-/-}$ mice.

In situ proximity ligation assays (PLA)

This technique is based on the use of oligonucleotide-conjugated antibodies, ligation of oligonucleotides by a bridging probe in a proximity-dependent manner, rolling-circle amplification, and visualization by complementary fluorescent probes (Söderberg et al., 2008). DAT–DAT interaction and DAT interactions with D_3R, D_2R and α-synuclein were studied using the Duolink II in situ PLA detection kit (Sigma) following the manufacturer's instructions. Striatal sections were obtained as described for immunohistochemistry, placed on glass slides, and incubated (1 h, 37 °C) with the blocking solution in a preheated humidity chamber. For the study of DAT–D_3R, DAT–D_2R and DAT–α-synuclein interactions, sections were incubated overnight at 4 °C with goat polyclonal anti-DAT antibody (1:200; Santa Cruz Biotechnology) and one of the following antibodies in the antibody diluent: rabbit polyclonal anti-D_3R antibody (1:200, Invitrogen), rabbit polyclonal anti-D_2R antibody (1:200; Millipore) and rabbit polyclonal anti-α-synuclein antibody (1:200, Santa Cruz Biotechnology). After several rinses in TBST (250 mM NaCl, 50 mM Tris, pH 7.4, and 0.05% Tween20), sections were incubated (2 h, 37 °C) with PLA probes detecting goat and rabbit or mouse antibodies (Duolink II plus PLA probe anti-goat and Duolink II minus PLA probe anti-mouse or anti-rabbit). Thereafter, samples were processed for ligation, amplification, and detection as described by the manufacturer. For the study of DAT–DAT interactions, sections were incubated with two anti-DAT antibodies directed to the C-terminus (1:200 rabbit polyclonal anti-DAT and 1:200 goat-polyclonal anti-DAT, Santa Cruz Biotechnology) and PLA probes detecting rabbit (plus) and goat (minus) antibodies. It should be noted that the use of

two antibodies directed to the same protein domain in the study of homodimers provides more specificity to the assay than the use of antibodies against two different domains because the first combination prevents the formation of PLA signals (oligonucleotide coupling) within a single DAT molecule. However, this combination also reduces assay sensitivity because the same antibody, and the same probe (minus or plus), may bind to the two partners of a DAT dimer, which is consequently not detected. For negative controls, one of the primary antibodies was substituted by non-immune goat, rabbit or mouse IgG, resulting in negative staining. Some sections were additionally processed for tyrosine hydroxylase (TH, the rate-limiting enzyme in dopamine synthesis) immunofluorescence by using a mouse monoclonal (1:4000, Sigma) or a rabbit polyclonal (1:1000, Millipore) anti-TH antibody. Samples were mounted using the mounting medium with DAPI and examined under a confocal laser scanning microscopy system (Olympus FV1000, Hamburg, Germany). Images were acquired in Z-stack mode (8.5 μm total thickness, 4 z-steps). Fluorescent PLA point-like signals were quantified, in number and size, in at least 12 striatal regions (400 μm × 400 μm) from 5 different mice per experimental group for each pair of primary antibodies, by using the ImageJ standard program.

Statistics

Mathematical analysis was performed using the one way ANOVA followed by the Tukey honest test for multiple post hoc comparisons. Analysis was performed using the Statistica program (Statsoft; Tulsa, U.S.A.). The degree of freedom in all comparisons was 1 (intergroup) and 8 (intragroup). A level of $p < 0.05$ was considered as critical for assigning statistical significance. Data are expressed as mean ± standard error of the mean.

Results

Pramipexole induces a decrease in DA uptake without changes in DAT expression levels

As mentioned in the Material and methods section, nomifensine-sensitive DA uptake was used to establish the lowest dose of PPX with bioactive effects on DAT. The analysis was performed in striatal synaptosomes of C57BL/6J mice receiving PPX in a dose range of 0.05–1.5 mg/kg/day for 6 days. A significant DA uptake decrease (47.8 ± 4.6%, $p < 0.01$; $F = 49.3$) was observed at doses ≥ 0.1 mg/kg/day (Fig. 1A), so this threshold dose was used in all experiments. The kinetics analysis of DAT (Fig. 1B) revealed a 79% increase in the K_m of treated mice with respect to that of untreated ones (52.6 ± 7.7 vs. 29.0 ± 4.1 nM, $n = 10$), but no changes were detected in V_{max} (sham, 25.4 ± 4.2; PPX, 24.8 ± 5.5 pmol DA/min/mg protein, $n = 10$). This suggests that differences in DA uptake are due to a reduction in DA affinity rather than to a decrease in the number of DA uptake sites. DA uptake returned to normal levels 5 days after PPX withdrawal (Fig. 1A).

The striatal expression of DAT was studied by immunohistochemistry and western-blot in whole striatal extracts and synaptosomal plasma membranes obtained from avidin-absorbed biotinylated surface proteins. As shown in Figs. 1C–F, PPX (0.1 mg/kg, 6 days) did not modify the DAT immunolabeling pattern and expression in whole striatal extracts. Furthermore, no DAT expression changes were detected at the plasma membrane level (Fig. 1G). An additional group of C57BL/6J mice received PPX for 21 days and was sacrificed on day 22 (Fig. 1H). Changes in DA uptake were similar to those measured in mice treated for 6 days and no changes in DAT expression were detected. Collectively, these data indicate that a prolonged PPX treatment induces DA uptake decrease without changes in the expression levels and subcellular distribution of DAT.

The effect of pramipexole on DAT is D_3R-mediated and D_2R-independent

In order to elucidate whether the DA uptake decrease induced by PPX is D_3R-mediated, $D_3R^{-/-}$ mice were also treated with PPX, and an additional C57BL/6J experimental group received the selective D_3R antagonist NGB2904 (1 mg/kg i.p.) 30 min before each PPX injection. As shown in Fig. 2A, both genetic D_3R deprivation and pretreatment with NGB2904 completely blocked the DA uptake decrease induced by PPX ($p < 0.01$; $F = 23.5$), indicating that this is a D_3R-mediated effect.

The possible involvement of the D_2R in the PPX effect was investigated using both a selective D_2R antagonist L741,626 in C57BL/6J mice, and $D_2R^{-/-}$ mice (Fig. 2B). L741,626 (1 mg/kg s.c.) administration 30 min before each PPX injection did not reverse the DA uptake decrease induced by PPX in C57BL/6J mice. With respect to the study in $D_2R^{-/-}$ mice, it should be noted that the basal DA uptake in both $D_2R^{-/-}$ mice and their wild-type littermates was 39% lower than in C57BL/6J mice (D_2R WT vs. C57BL/6J, 38.7 ± 3.1%, $p < 0.01$, $F = 37.2$; $D_2R^{-/-}$ vs.

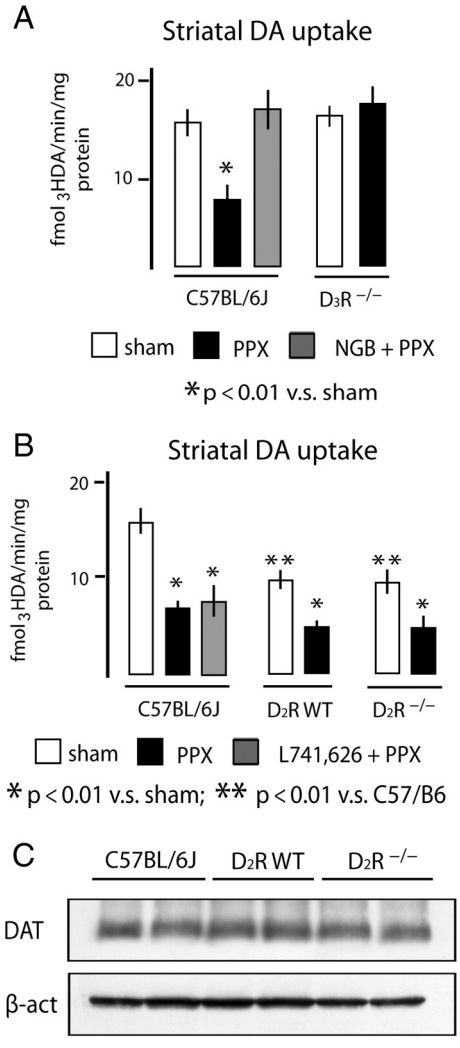

Fig. 2. Involvement of D_3R (A) and D_2R (B, C) in the effect of PPX on DA uptake. (A, left) The DA uptake decrease induced by PPX in C57BL/6J mice is inhibited by the injection of the selective D_3R antagonist NGB2904 (1 mg/kg) 30 min before each PPX injection (NGB + PPX). (A, right) PPX induced no DA uptake changes in $D_3R^{-/-}$ mice. (B, left) The DA uptake decrease induced by PPX in C57BL/6J mice is not reversed by the injection of the selective D_2 receptor antagonist L741,626 (1 mg/kg) 30 min before each PPX injection (L741,626 + PPX). (B, center and right) Basal DA uptake in $D_2R^{-/-}$ mice is similar to that in their wild-type littermates (D_2RWT) but lower than that in C57BL/6J mice. PPX induced similar DA uptake decrease in both strains (D_2RWT and $D_2R^{-/-}$). (C) DAT expression in the striatum of C57BL/6J, D_2RWT and $D_2R^{-/-}$ mice, showing no differences between them. β-act, β-actin.

C57BL/6J, 39.6 ± 4.0%, $p < 0.01$; $F = 29.9$; Fig. 2B), although no DAT expression differences were detected between them (Fig. 2C, also Granado et al., 2011). Consistent with that found in C57BL/6J mice receiving L741,626 pretreatment, PPX induced a significant decrease of DA uptake in both $D_2R^{-/-}$ (41.9 ± 3.3% vs. sham, $p < 0.01$, $F = 12.8$) and their wild-type littermates (40.4 ± 6.1% vs. sham, $p < 0.01$, $F = 19.5$). Therefore, the DA uptake decrease induced by PPX is a D_3R-mediated and D_2R-independent effect.

Pramipexole promotes the formation of DAT dimers and DAT-associated protein complexes

The absence of a decline in DAT levels in whole striatal extracts and in its densities in the synaptosomal membrane fraction suggests that mechanisms other than DAT expression down-regulation or internalization are responsible for the PPX-induced DA uptake decrease. Bearing in mind that DAT may be expressed in the form of dimers (Baucum et al., 2004; Hastrup et al., 2001), and that its activity is critically dependent on its association with protein partners (Ericksen et al., 2010; Torres, 2006), changes in DAT-associated protein complex were investigated by different procedures. Striatal synaptosomes were first analyzed under non-reducing conditions. As shown in Fig. 3A, apart from a solid band at 65–80 kDa corresponding to the glycosylated monomeric DAT form (Afonso-Oramas et al., 2009), a weak band was also detected in untreated mice at ~150 kDa, i.e. a molecular weight corresponding to DAT dimer. After PPX treatment, the 65–80 kDa band became weaker in labeling intensity (a decrease of 47.2 ± 7.3% with respect to Sham, $p < 0.01$, $F = 11.2$) and that at ~150 kDa became more intense (an increase of 75.9 ± 6.1% with respect to Sham, $p < 0.01$, $F = 14.6$) in C57BL/6J mice. In contrast, PPX treatment of $D_3R^{-/-}$ mice did not alter the profile of DAT immunoreactivity in SDS-PAGE, suggesting that D_3R stimulation promotes DAT dimer formation. To confirm dimer formation, striatal sections were processed for DAT–DAT in situ PLA. As mentioned in the Material and methods section, the use of two antibodies against the same DAT domain (C-terminus) increases specificity but also reduces the sensitivity of the assay. DAT–DAT PLA signals were detected around striatal cells of untreated C57BL/6J and $D_3R^{-/-}$ mice (Figs. 3B, C, left), which supports the idea that the weak ~150 kDa band found under non-reducing conditions corresponds, at least in part, to DAT dimers. The PLA dot count revealed an increase of 48.8% in number after PPX treatment ($p < 0.01$, $F = 18.8$, Fig. 3B) in C57BL/6J mice. The size of the PLA dots was also significantly larger in PPX-treated C57BL/6J mice, with an average size triple that of untreated mice (87.3 ± 8.1 vs. 30.1 ± 2.3 pixels). However, no changes were found in $D_3R^{-/-}$ mice (Fig. 3C, right), indicating that PPX promotes DAT dimer formation by a D_3R mediated mechanism, with large-sized dots probably corresponding to two or more PLA signals localized close to each other.

In addition to its ability to form dimers, DAT can interact with a number of proteins, including the D_2R (Lee et al., 2007) and α-synuclein

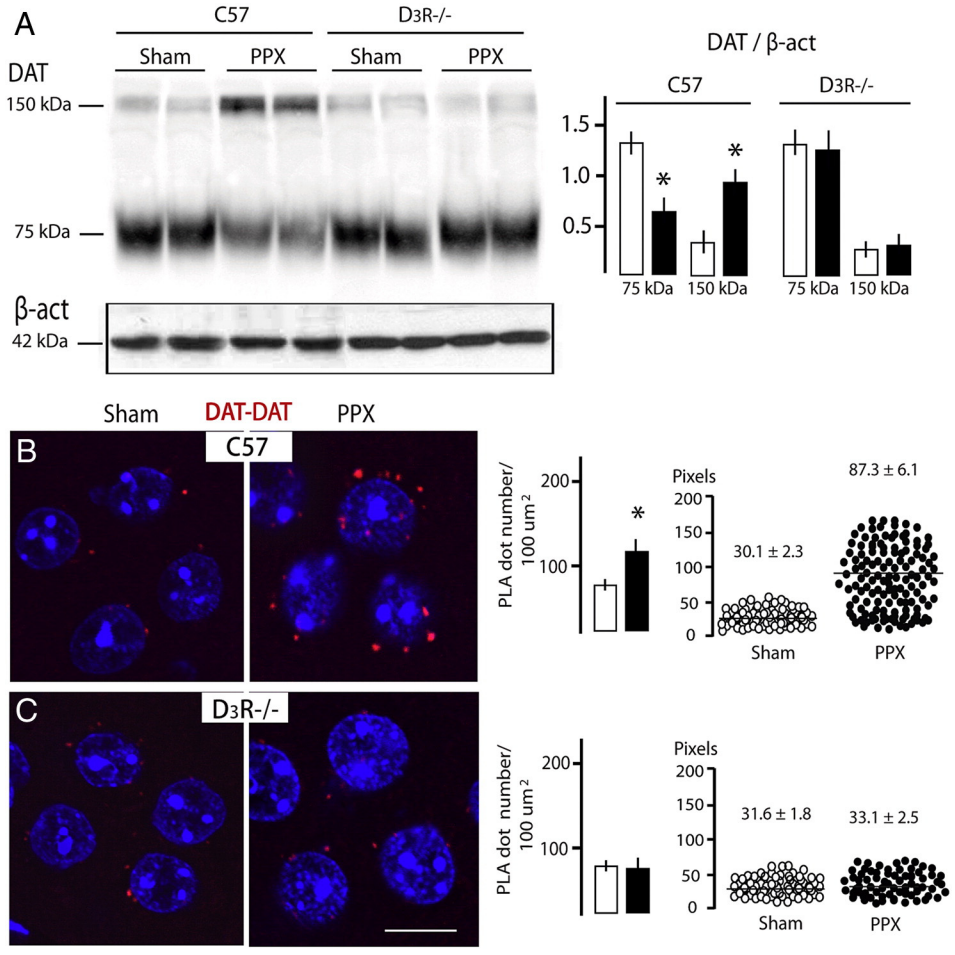

Fig. 3. Pramipexole induces the formation of DAT dimers. (A) Striatal samples blotted under non-reducing conditions revealed a weak band at 150 kDa, besides that a 65–80 kDa, in sham treated mice (Sham, lanes 1 and 2). The high weight band was significantly more intense in labeling and that at 65–80 kDa became weaker after treatment (PPX, 0.1 mg/kg/day, 6 days) in C75BL/6J mice (lanes 3 and 4), but not in $D_3R^{-/-}$ mice (lanes 5–8). (B, C) DAT–DAT in situ proximity ligation assay (PLA) showing an increase in both number and size of PLA dots after PPX treatment in C57BL/6J mice (B) but not in $D_3R^{-/-}$ mice (C). The quantitative analysis was performed in 5 animals per group (see the Material and methods section). In the size diagrams (on the right), the numbers indicate the average size (pixels) of PLA signals. Each dot corresponds to 8 PLA signals in a field of 200 μm² from a representative animal. β-act, β-actin. Scale bar in C (for B and C), 5 μm.

(Wersinger and Sidhu, 2003). We thus examined the impact of prolonged PPX treatment upon D_2R/DAT and α-synuclein/DAT interactions. As shown in Fig. 4A, DAT co-immunoprecipitated with D_2R in both C57BL/6J and $D_3R^{-/-}$ untreated mice, however PPX induced an increase in DAT co-immunoprecipitation with D_2R in C57BL/6J ($p < 0.01$, $F = 17.7$) but not in $D_3R^{-/-}$. Co-immunoprecipitation control experiments were performed in $D_2R^{-/-}$ mice. Striatal sections processed for DAT–D_2R PLA showed pericellular PLA signals, and combination with TH immunofluorescence corroborated their localization in DA-terminals of sham and PPX-treated mice (Fig. 4B). As described for DAT–DAT interaction, both the number and the size of DAT–D_2R PLA dots increased after PPX treatment in C57BL/6J mice (Figs. 4B–D). However, no differences were found in the number and size of PLA dots between PPX + NGB2904 treated and untreated mice (Figs. 4C, D), and between PPX treated and untreated $D_3R^{-/-}$ mice (Fig. 4E). The virtual absence of large-sized dots in untreated and PPX + NGB2904-treated C57BL76J mice, and in PPX treated $D_3R^{-/-}$ mice, indicates that the effect is D_3R-specific. With respect to the study of DAT–α-synuclein interactions, DAT–α-synuclein co-immunoprecipitation and the count of point-like DAT–α-synuclein PLA signals (Figs. 5 A–C) showed no differences

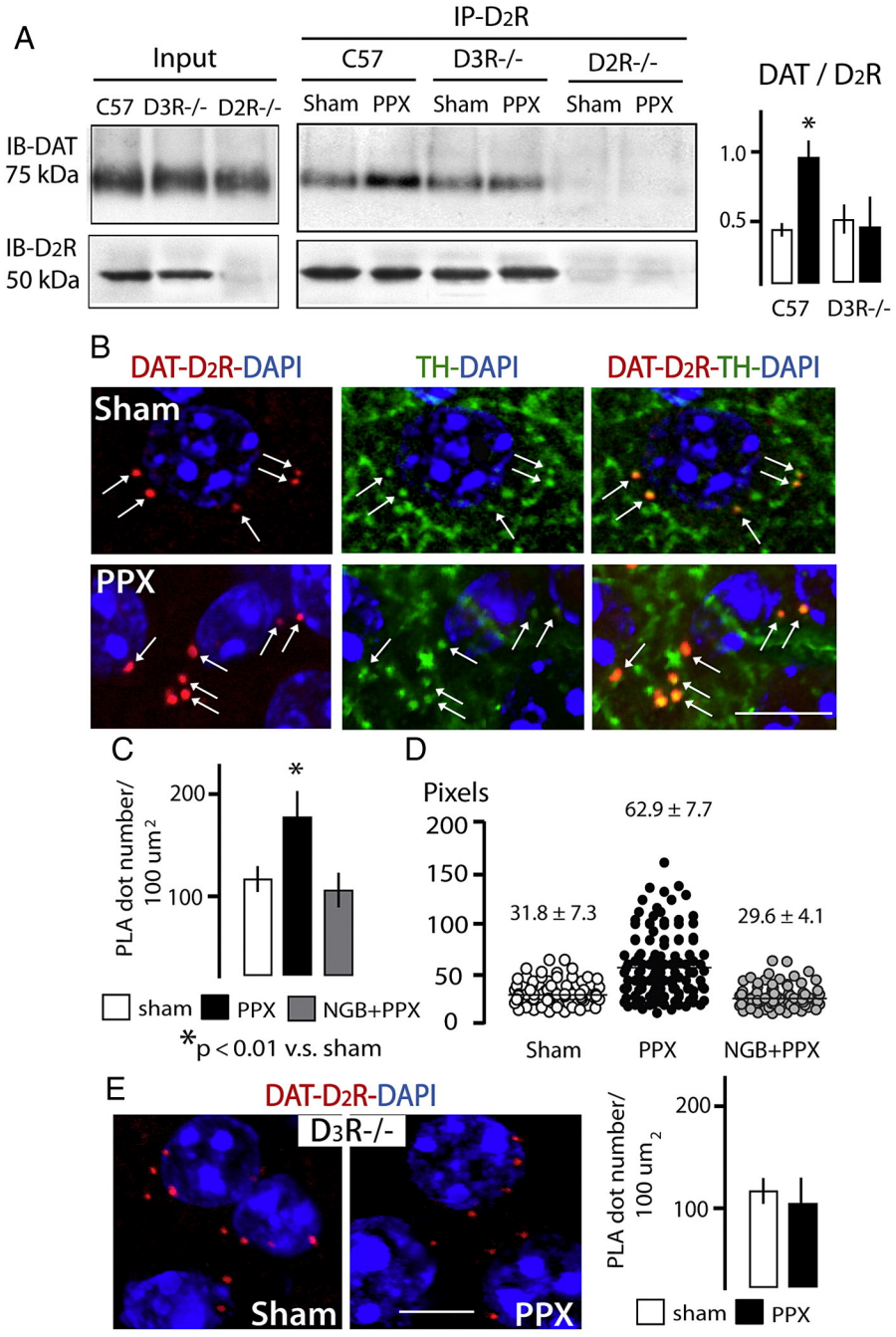

Fig. 4. Pramipexole modifies the DAT–D_2R interaction. (A) Immunoprecipitation for D_2R (IP-D_2R) and immunoblotting for DAT (IB-DAT) and D_2R (IB-D_2R). Co-immunoprecipitated DAT increases after PPX treatment (PPX; 0.1 mg/kg/day, 6 days) in C57BL/6J mice, but not in $D_3R^{-/-}$ mice. Control experiments were performed in $D_2R^{-/-}$ mice. (B) PLA for DAT and D_2R (left), and TH immunofluorescence (center) in the striatum of untreated (Sham) and PPX-treated (PPX) C57BL/6J mice. Arrows indicate that DAT–D_2R PLA signals (red) localize in DA-terminals (green). (C, D) Quantitative analysis of the number (C) and size (D) of PLA dots in C57BL/6J mice. One can see that the number and size of PLA dots increase in PPX treated mice, but not in those receiving NGB + PPX. (E) PLA for DAT and D_2R in $D_3R^{-/-}$ mice showing no changes in number and size after PPX treatment. IgG in (A), control immunoprecipitation using non-immune IgG. In (C–E), n = 5 animals/group. In the size diagram (D), the numbers indicate the average size (pixels) of PLA signals. Each dot corresponds to 8 PLA signals in a field of 200 μm^2 from a representative animal. Scale bar in B (for the six micrographs) and E (for both micrographs), 5 μm.

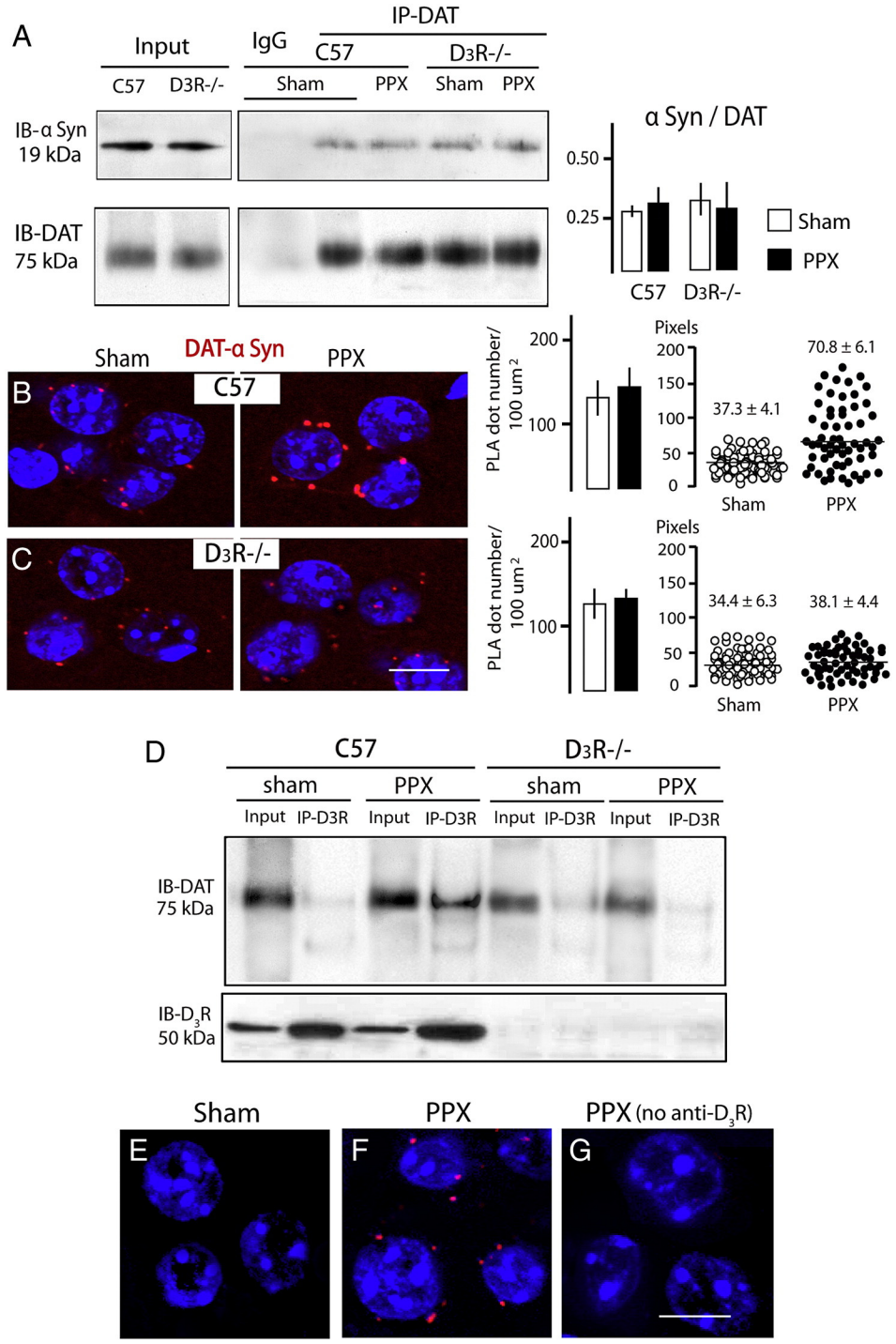

Fig. 5. (A–C) Pramipexole modifies DAT-α synuclein interaction. (A) Immunoprecipitation for DAT (IP-DAT) and immunoblotting for α-synuclein (IB-α Syn) and DAT (IB-DAT). No changes were found in the levels of co-immunoprecipitated α-synuclein after PPX treatment (PPX; 0.1 mg/kg/day, 6 days) in both C57BL/6J and $D_3R^{-/-}$ mice. (B, C) PLA for DAT and α-synuclein showing that after PPX treatment the average size of PLA dots increases in C57BL/6J mice (B) but not in $D_3R^{-/-}$ mice (C). No changes were detected in the PLA dot number in both strains. (D–G) Pramipexole induces physical interaction between D_3R and DAT. (D) Immunoprecipitation for D_3R (IP-D_3R) and immunoblotting for DAT (IB-DAT) and D_3R (IB-D_3R). DAT was co-immunoprecipitated in PPX-treated mice (0.1 mg/kg/day, 6 days) but not in sham-treated mice. Control experiments were performed in $D_3R^{-/-}$ mice. (E–G) PLA for D_3R and DAT. PLA dots were detected in PPX-treated mice (F) but not in sham-treated mice (E) and in PPX-treated mice when one of the primary antibodies was omitted (G). In (B, C), n = 5 animals/group. In the size diagram, the numbers indicate the average size (pixels) of PLA signals. Each dot corresponds to 8 PLA signals in a field of 200 μm^2 from a representative animal. IgG in (A, D), control immunoprecipitation using non-immune IgG; no pp in (d), control immunoprecipitation omitting protein extracts. Bar in C (for B and C) and in G (for E–G), 5 μm.

between untreated and PPX-treated C57BL/6J or $D_3R^{-/-}$ mice. However, the average dot size doubled in C57BL/6J (Fig. 5B) but not in $D_3R^{-/-}$ mice (Fig. 5C).

In line with previous findings which identified D_2R as one of the DAT partners (Lee et al., 2007) and the structural homology between D_2R and D_3R (Platania et al., 2012; Wang et al., 2010), we then examined whether the D_3R also interacts with DAT. Data arising from co-immunoprecipitation and PLA (Figs. 5D–G) revealed no DAT–D_3R physical interaction in the striatum of untreated mice. However, after PPX treatment, DAT was immunoprecipitated with D_3R (Fig. 5D) and DAT–D_3R PLA point-like signals appeared around striatal neurons (Fig. 5F). DAT was not co-immunoprecipitated in $D_3R^{-/-}$ mice, and PLA signals

were not detected in PPX treated mice when one of the primary antibodies (anti-DAT or anti-D_3R) was substituted by non-immune serum (Fig. 5G). These data indicate that D_3R is not a constitutive partner of DAT but that PPX induces their interaction.

Discussion

Together with a decrease in DA uptake, prolonged treatment with the preferential D_3R agonist PPX promotes DAT dimer formation and DAT interaction with some of its protein partners, including the D_3R receptor itself and the D_2R. The increase in DAT–D_2R co-immunoprecipitation and in DAT–D_2R, DAT–α-synuclein and DAT–DAT PLA signals indicates that DAT interactions undergo modifications as a consequence of prolonged PPX treatment, forming clusters of larger multiprotein complexes. The absence of DAT-associated complexes in D_3R deficient mice indicates that the effect is D_3R-dependent. The analysis of PLA signals was based on two parameters: number and size. While dot number is widely used as an index of the number of protein–protein interactions, and has even been proposed for clinical applications (Aranguren et al., 2013; Aubele et al., 2010), dot size has not yet been afforded much attention. Bearing in mind dot size uniformity in sham-treated mice, the substantial increase observed after PPX treatment is an interesting observation that might reflect small clusters of PLA signals. However, there is currently no direct evidence for a relationship between dot size and the number of interactions. Accordingly, this finding must be interpreted with caution awaiting further characterization.

Notably, high molecular weight DAT-associated complexes were previously described in rats after multiple administration of methamphetamine or striatal injection of 6-hydroxydopamine (Baucum et al., 2004; Hadlock et al., 2009). Furthermore, DAT–α-synuclein aggregates, together with increased DAT and α-synuclein cellular levels and changes in their subcellular distribution, were also found in a mouse model of Parkinson's disease based on SYN_{1-120} overexpression (Bellucci et al., 2011). Thus, oxidative stress and disruption of dopaminergic transmission might also underlie the formation of high molecular weight DAT-associated complexes. However, our data show that prolonged D_3R stimulation does not affect α-synuclein expression, and DAT levels and its functional distribution were also unchanged, even after 21 days of treatment. This suggests that dopaminergic transmission is preserved in PPX-treated mice, and that the formation of high molecular weight DAT complexes may occur in dopaminergic neurons to regulate DAT activity in response to different conditions: these complexes are not necessarily toxic, nor do they necessarily lead to protein aggregation. Interestingly, data from cellular and animal models of Parkinson's disease indicate that D_3R agonists have the ability to counteract the formation of α-synuclein inclusions (Bellucci et al., 2008; Kakimura et al., 2001). Thus, it is possible that PPX promotes the turnover of DAT and its protein partners, maintaining their cellular levels within the normal range even when forming high molecular weight multiprotein complexes.

It is well-known that dopaminergic neurons display adaptive responses aimed at normalizing DA neurotransmission following prolonged administration of DA agonists. These include changes in firing rate (Chernoloz et al., 2009), and phosphorylation of active DA receptors, resulting in their desensitization and internalization (for review see Evron et al., 2012). Further studies have implicated DAT in adaptive responses: while acute D_3R stimulation enhanced DA uptake (Zapata et al., 2007; Zapata and Shippenberg, 2005), prolonged agonist exposure for 30 min in in vitro studies (Zapata et al., 2007), or for a few days in mice (Joyce et al., 2004), decreased DA uptake. Our findings agree with this notion and indicate that adaptive mechanisms in response to prolonged PPX treatment involve DAT protein–protein interactions. Moreover, using $D_3R^{-/-}$ mice, we found that functional as well as biochemical DAT changes require D_3R. The fact that DAT is also regulated by D_2R (Bolan et al., 2007; Bowton et al., 2010; Lee et al., 2007) raises the possibility of a role of D_2R in these events. However, as our results show, the decrease in DA uptake and the formation of multiprotein complexes upon prolonged PPX administration were preserved in $D_2R^{-/-}$ mice, suggesting that both effects are D_2R-independent. As such, D_3R agonists may need D_2R to induce the acute increase in DAT activity, as suggested by Zapata and Shippenberg (2005), but not for the decrease in DAT activity and changes in DAT proteome elicited after prolonged administration.

The present study reveals that the maximal velocity of DA uptake (which directly correlates with the number of DAT active sites) was not affected by PPX, while K_m (which inversely correlates with DAT affinity for DA) increased. Therefore, one can assume that most DAT, with reduced affinity, is retained at the plasma membrane in PPX-treated animals, while internalization and subsequent clearance, considered as standard mechanisms of DAT regulation (Miranda and Sorkin, 2007; Mortensen and Amara, 2003), are not of major significance in this paradigm. We also demonstrated here that, unlike the D_2 autoreceptor (Lee et al., 2007), the D_3 autoreceptor is not a constitutive component of the DAT-associated protein complex, but that its interaction with DAT is induced by PPX. Interestingly, Min et al. (2013) have recently found that in contrast to what happens to most G protein-coupled receptors, including D_2R, during agonist-induced desensitization, most D_3R moves towards hydrophobic domains within the plasma membrane without translocation to intracellular compartments. Hence, the fact that DAT is retained in the plasma membrane after prolonged PPX treatment may be a consequence of both its interaction with D_3 autoreceptor and the anchoring of this to membrane hydrophobic domains.

An intriguing question arising from these findings is whether DAT may also be modulated through physiological actions of endogenously-released DA at D_3 autoreceptors. While current data agree on the critical role of D_2 autoreceptors in basal DA uptake regulation (Bolan et al., 2007; Ford, 2014; Lee et al., 2007), the participation of D_3 autoreceptors remains controversial. Our results, coinciding with those from Zapata et al. (2007), Joseph et al. (2002), showed no differences in the basal DA uptake between D_3R KO mice and their wild type littermates, suggesting that D_3R is probably not implicated in basal DAT regulation. However, Joyce et al. (2004) found reduced Vmax in DA uptake of D_3R KO mice, and Zapata and Shippenberg (2002) reported a reduced rate of DA clearance in striatal tissue of Swiss Webster mice pre-incubated with a D_3R antagonist, suggesting that D_3R participates in the physiological regulation of DAT. The fact that DA affinity for D_3R is higher than for D_2R (Sokoloff et al., 1990; Freedman et al., 1994; Platania et al., 2012) also indicates that DAT-D_3R interactions likely operate within the physiological range of extracellular levels of DA, though this possibility needs to be directly confirmed.

Even though the therapeutic use of PPX in Parkinson's disease to relieve motor symptoms is linked to its postsynaptic actions (Millan, 2010), some studies suggest that PPX and other DA agonists exert neuroprotective effects, related to both recruitment of D_3 autoreceptors and non-dopaminergic actions such as antioxidant properties (Albrecht and Buerger, 2009; Joyce and Millan, 2007). Bearing in mind the role of DAT in the pathogenesis of Parkinson's disease, increasing intracellular levels of DA and consequently the oxidative burden, the dual time-dependent effect of D_3R agonists on DAT may impact the vulnerability of dopaminergic neurons in two different ways. On the one hand, acute exposure to agonists promotes DAT recruitment at the plasma membrane and increased DA uptake through G-protein mediated mechanisms (Zapata et al., 2007). On the other hand, consistent with the fact that prolonged exposure to agonists induces D_3 autoreceptor desensitization (Min et al., 2013), Joyce et al. (2004) proposed that sustained treatment with PPX might protect DA-cells by a dopaminergic mechanism inducing DAT down-regulation. Our findings support this idea in part by confirming the decrease of DA uptake, but differ in the mechanistic foundation by suggesting that the effect of PPX is mediated by a physical interaction between the D_3 autoreceptor and DAT. Likewise, bearing in

mind the implication of DAT and D_3R in the pathogenesis of depression (Amsterdam et al., 2012; Sokoloff et al., 2006; Zahniser and Sorkin, 2009), D_3 autoreceptor-DAT interaction might also be involved in the antidepressant effect proposed for PPX (Cusin et al., 2013), contributing to maintain high DA levels in the extracellular space.

The serotonin transporter (SERT) is also a widely studied Na^+/Cl^--dependent transporter that shares biochemical properties and regulatory mechanisms with DAT. For example, like DAT, it has a natural propensity to form homo-oligomers (Anderluh et al., 2014; Hastrup et al., 2001; Schmid et al., 2001), and its trafficking and internalization involve presynaptic and membrane proteins which also interact with DAT (Carneiro and Blakely, 2006; Chanrion et al., 2007; Ericksen et al., 2010; Torres, 2006). In addition, SERT is regulated by 5-HT autoreceptors in a time-dependent manner. While acute administration of SERT inhibitor antidepressants activates terminal $5\text{-}HT_{1B}$ autoreceptors, reducing 5-HT synthesis and release, their chronic administration down-regulates $5\text{-}HT_{1B}$ mRNA in presynaptic neurons as an adaptive response directed at increasing serotoninergic transmission (Neumaier et al., 1996). However, ligand-induced interactions between 5-HT autoreceptors and SERT (reminiscent of D_3R–DAT interaction) have not yet been reported, suggesting that there may be differences in long-term adaptive responses between DAT versus SERTs and other classes of transporter, though this awaits further elucidation.

In summary, we describe a new pattern of inducible protein–protein interaction involving an autoreceptor and the corresponding neurotransmitter transporter. The data suggest that the changes seem to occur as an adaptive mechanism to modulate DA transmission via the transporter upon prolonged exposure to an agonist. Further studies will be required to confirm the pertinence of these observations to the long-term effects of D_3R agonists in the management of psychiatric and neurological disorders.

Conflict of interest

The authors declare no conflict of interest.

Acknowledgments

This study was supported by the grants BFU2010-21130 and BFU2013-47242-R (Ministerio de Ciencia e Innovación) to T G-H, BFU2010-20664 (Ministerio de Ciencia e Innovación), PNSD, to R M, and the IMBRAIN project (FP7-REGPOT-2012-CT2012-31637-IMBRAIN), funded under the 7th Framework Programme (Capacities). J C-H was supported by a predoctoral fellowship from the Fundación Canaria de Investigación y Salud (ID54), J S-H was partially supported by the Agencia Canaria de Investigación, Innovación y Sociedad de la Información (SE-10/19), and P B-C was supported by a grant from the Campus de Excelencia Internacional (FEDER, ULL, CEI 10/00018-EDU/903/2010). The authors wish to thank Dr. Philippe Marin at the University of Monpellier, France, for his feedback and helpful comments in the preparation of this manuscript.

References

Accili, D., Fishburn, C.S., Drago, J., Steiner, H., Lachowicz, J.E., Park, B.H., Gauda, E.B., Lee, E.J., Sibley, D.R., Gerfen, C.R., Westphal, H., Fuchs, S., 1996. A targeted mutation on the D3 dopamine receptor gene is associated with hyperactivity in mice. Proc. Natl. Acad. Sci. U. S. A. 93, 1945–1949. http://dx.doi.org/10.1073/pnas.93.5.1945.

Afonso-Oramas, D., Cruz-Muros, I., Alvarez de la Rosa, D., Abreu, P., Giraldez, T., Castro-Hernández, J., Salas-Hernández, J., Lanciego, J.L., Rodríguez, M., González-Hernández, T., 2009. Dopamine transporter glycosylation correlates with the vulnerability of midbrain dopaminergic cells in Parkinson's disease. Neurobiol. Dis. 36, 494–508. http://dx.doi.org/10.1016/j.nbd.2009.09.002.

Afonso-Oramas, D., Cruz-Muros, I., Barroso-Chinea, P., Álvarez de la Rosa, D., Castro-Hernández, J., Salas-Hernández, J., Giráltez, T., González-Hernández, T., 2010. The dopamine transporter is differentially regulated after dopaminergic lesion. Neurobiol. Dis. 40, 518–530. http://dx.doi.org/10.1016/j.nbd.2010.07.012.

Albrecht, S., Buerger, E., 2009. Potential neuroprotection mechanisms in PD: focus on dopamine agonist pramipexole. Curr. Med. Res. Opin. 25, 2977–2987. http://dx.doi.org/10.1185/03007990903364954.

Amsterdam, J.D., Newberg, A.B., Soeller, I., Shults, J., 2012. Greater striatal dopamine transporter binding in major depressive disorder. J. Affect. Disord. 141, 425–431. http://dx.doi.org/10.1016/j.jad.2012.03.007.

Anderluh, A., Klotzsch, E., Reismann, A.W., Brameshuber, M., Kudlacek, O., Newman, A.H., Sitte, H.H., Schütz, G.J., 2014. Single molecule analysis reveals coexistence of stable serotonin transporter monomers and oligomers in the live cell plasma membrane. J. Biol. Chem. 289, 4387–4394. http://dx.doi.org/10.1074/jbc.M113.531632.

Aranguren, X.L., Beerens, M., Ludyga, N., Braselmann, H., Feuchtinger, A., Taylor, K.J., Lindner, K., Auer, G., Stering, K., Höfler, H., Schmitt, M., Bartlett, J.M., 2010. In situ quantification of HER2-protein tyrosine kinase 6 (PTK6) protein–protein complexes in paraffin sections from breast cancer tissues. Br. J. Cancer 103, 663–667. http://dx.doi.org/10.1038/sj.bjc.6605836.

Baucum II, A.J., Rau, K.S., Riddle, E.L., Hanson, G.R., Fleckenstein, A.E., 2004. Methamphetamine increases dopamine transporter higher molecular weight complex formation via a dopamine- and hyperthermia-associated mechanism. J. Neurosci. 24, 3436–3443. http://dx.doi.org/10.1523/JNEUROSCI. 0387-04.2004.

Bellucci, A., Collo, G., Sarnico, I., Battistin, L., Missale, C., Spano, P., 2008. Alpha-synuclein aggregation and cell death triggered by energy deprivation and dopamine overload are counteracted by D_2/D_3 receptor activation. J. Neurochem. 106, 560–577. http://dx.doi.org/10.1111/j.1471-4159.2008.05406.x.

Bellucci, A., Navarria, L., Falarti, E., Zaltieri, M., Bono, F., Collo, G., Spillantini, M.G., Missale, C., Spano, P., 2011. Redistribution of DAT/ α-synuclein complexes visualized by "in situ" proximity ligation assay in transgenic mice modelling early Parkinson's disease. PLoS One 6, e27959. http://dx.doi.org/10.1371/journal.pone.0027959.

Bolan, E.A., Kivell, B., Jaligam, V., Oz, M., Yajanthi, L.D., Han, Y., Sen, N., Urizar, E., Gomes, I., Devi, L.A., Ramamoorthy, S., Javitch, J.A., Zapata, A., Shippenberg, T.S., 2007. D_2 receptors regulate dopamine transporter function via an extracellular signal-regulated kinases 1 and 2-dependent and phosphoinositide 3 kinase-independent mechanism. Mol. Pharmacol. 71, 1222–1232. http://dx.doi.org/10.1124/mol.106.027763.

Bowton, E., Saunders, C., Erreger, K., Sakrikar, D., Mathies, H., Sen, N., Jessen, T., Colbran, R.J., Caron, M.G., Javitch, J.A., Blakely, R.D., Galli, A., 2010. Dysregulation of dopamine transporter via D_2 autoreceptor triggers anomalous dopamine efflux associated with attention-deficit hyperactivity disorder. J. Neurosci. 30, 6048–6057. http://dx.doi.org/10.1523/JNEUROSCI. 5094-09.201.

Carneiro, A.M., Blakely, R.D., 2006. Serotonin-, protein kinase C-, and Hic-5-associated redistribution of the platelet serotonin transporter. J. Biol. Chem. 281, 24769–24780. http://dx.doi.org/10.1074/jbc.M603877200.

Chanrion, B., Mannoury la Cour, C., Bertaso, F., Lerner-Natoli, M., Freissmuth, M., Millan, M.J., Bockaert, J., Marin, P., 2007. Physical interaction between the serotonin transporter and neuronal nitric oxide synthase underlies reciprocal modulation of their activity. Proc. Natl. Acad. Sci. U. S. A. 104, 8119–8124. http://dx.doi.org/10.1073/pnas.0610964104.

Chen, R., Daining, C.P., Sun, H., Fraser, R., Stokes, S.L., Leitges, M., Gnegy, M.E., 2013. Protein kinase Cβ is a modulator of the dopamine D2 autoreceptor-activated trafficking of the dopamine transporter. J. Neurochem. 125, 663–672. http://dx.doi.org/10.1111/jnc.12229.

Chernoloz, O., El Mansari, M., Blier, P., 2009. Sustained administration of pramipexole modifies the spontaneous firing of dopamine, norepinephrine, and serotonin neurons in the rat brain. Neuropsychopharmacology 34, 651–661. http://dx.doi.org/10.1038/npp.2008.114.

Collins, G.T., Newman, A.H., Grundt, P., Rice, K.C., Husbands, S.M., Chauvignac, C., Chen, J., Wang, S., Woods, J.H., 2007. Yawing and hypothermia in rats: effects of dopamine D3 and D2 agonists and antagonists. Psychopharmacology 193, 159–170. http://dx.doi.org/10.1007/s00213-007-0766-3.

Collo, G., Bono, F., Cavalleri, L., Plebani, L., Merlo Pich, E., Millan, M.J., Spano, P.F., Missale, C., 2012. Pre-synaptic dopamine D (3) receptor mediates cocaine-induced structural plasticity in mesencephalic dopaminergic neurons via ERK and Akt pathways. J. Neurochem. 120, 765–778. http://dx.doi.org/10.1111/j.1471-4159.2011.07618.x.

Cruz-Muros, I., Afonso-Oramas, D., Abreu, P., Perez-Delgado, M.M., Rodriguez, M., Gonzalez-Hernandez, T., 2009. Aging effects on the dopamine transporter expression and compensatory mechanisms. Neurobiol. Aging 30, 973–986. http://dx.doi.org/10.1016/j.neurobiolaging.2007.09.009.

Cusin, C., Iovieno, N., Iosifescu, D.V., Nierenberg, A.A., Fava, M., Rush, A.J., Perlis, R.H., 2013. A randomized, double-blind, placebo-controlled trial of pramipexole augmentation in treatment-resistant major depressive disorder. J. Clin. Psychiatry 74, e636–e641. http://dx.doi.org/10.4088/JCP.12m08093.

Diaz, J., Pilon, C., Le Foll, B., Gros, C., Triller, A., Schwartz, J.C., Sokoloff, P., 2000. Dopamine D3 receptors expressed by all mesencephalic dopamine neurons. J. Neurosci. 20, 8677–8684 (Available on line at: http://www.jneurosci.org/content/20/23/8677.long).

Ericksen, J., Jorgensen, T.N., Gether, U., 2010. Regulation of dopamine transporter function by protein–protein interactions: new discoveries and methodological challenges. J. Neurochem. 113, 27–41. http://dx.doi.org/10.1111/j.1471-4159.2010.06599.x.

Evron, T., Daigle, T.L., Caron, M.G., 2012. GRK2: multiple roles beyond G protein-coupled receptor desensitization. Trends Pharmacol. Sci. 33, 154–164. http://dx.doi.org/10.1016/j.tips.2011.12.003.

Ford, C.P., 2014. The role of D2-autoreceptors in regulating dopamine neuron activity and transmission. Neuroscience 282C, 13–22. http://dx.doi.org/10.1016/j.neuroscience.2014.01.025.
Freedman, S.B., Patel, S., Marwood, R., Emms, F., Seabrook, G.R., Knowles, M.R., McAllister, G., 1994. Expression and pharmacological characterization of the human D3 dopamine receptor. J. Pharmacol. Exp. Ther. 268, 417–426.
Gonzalez-Hernandez, T., Barroso-Chinea, P., de la Cruz-Muros, I., Pérez-Delgado, M.M., Rodríguez, M., 2004. Expression of dopamine and vesicular monoamine transporters and differential vulnerability of mesostriatal dopaminergic neurons. J. Comp. Neurol. 479, 198–215. http://dx.doi.org/10.1002/cne.20323.
Granado, N., Ares-Santos, S., Oliva, I., O'Shea, E., Martin, E.D., Colado, M.I., Moratalla, R., 2011. Dopamine D2-receptor knockout mice are protected against dopamine neurotoxicity induced by methamphetamine or MDMA. Neurobiol. Dis. 42, 391–403. http://dx.doi.org/10.1016/j.nbd.2011.01.033.
Hadlock, G.C., Baucum II, A.J., King, J.L., Horner, K.A., Cook, G.A., Gibb, J.W., Wilkins, D.G., Hanson, G.R., Fleckenstein, A.E., 2009. Mechanisms underlying methamphetamine-induced dopamine transporter complex formation. J. Pharmacol. Exp. Ther. 329, 169–174. http://dx.doi.org/10.1124/jpet.108.145631.
Hadlock, G.C., Nelson, C.C., Baucum II, A.J., Hanson, G.R., Fleckenstein, A.E., 2011. Ex vivo identification of protein–protein interactions involving the dopamine transporter. J. Neurosci. Methods 196, 303–307. http://dx.doi.org/10.1016/j.jneumeth.2011.01.023.
Hastrup, H., Karlin, A., Javitch, J.A., 2001. Symmetrical dimer of the human dopamine transporter revealed by cross-linking Cys-306 at the extracellular end of the sixth transmembrane segment. Proc. Natl. Acad. Sci. U. S. A. 98, 10055–10060. http://dx.doi.org/10.1073/pnas.181344298.
Joseph, J.D., Wang, Y.M., Miles, P.R., Budygin, E.A., Picetti, R., Gainetdinov, R.R., Caron, M.G., Wightman, R.M., 2002. Dopamine autoreceptor regulation of release and uptake in mouse brain slices in the absence of D(3) receptors. Neuroscience 112, 39–49. http://dx.doi.org/10.1016/S0306-4522(02)00067-2.
Joyce, J.N., Millan, J.M., 2007. Dopamine D_3 receptor agonists for protection and repair in Parkinson's disease. Curr. Opin. Pharmacol. 7, 100–105. http://dx.doi.org/10.1016/j.coph.2006.11.004.
Joyce, J.N., Woolsey, C., Ryoo, H., Borwege, S., Hagner, D., 2004. Low dose pramipexole is neuroprotective in the MPTP model of Parkinson's disease, and downregulates the dopamine transporter via D_3 receptor. BMC Biol. 2, 1–12. http://dx.doi.org/10.1186/1741-7007-2-22.
Kakimura, J., Kitamura, Y., Takata, K., Kohno, Y., Nomura, Y., Taniguchi, T., 2001. Release and aggregation of cytochrome c and alpha-synuclein are inhibited by antiparkinsonian drugs, talipexole and pramipexole. Eur. J. Pharmacol. 417, 59–67. http://dx.doi.org/10.1016/S0014-2999(01)00902-5.
Kelly, M.A., Rubinstein, M., Asa, S.L., Zhang, G., Saez, C., Bunzow, J.R., Allen, R.G., Hnasko, R., Ben-Jonathan, N., Grandy, D.K., Low, M.J., 1997. Pituitary lactotroph hyperplasia and chronic hyperprolactinemia in dopamine D2 receptor-deficient mice. Neuron 19, 103–113. http://dx.doi.org/10.1016/S0896-6273(00)80351-7.
Kofarnus, M.N., Greedy, B., Husbands, S.M., Grundt, P., Newman, A.H., Woods, J.H., 2009. The discriminative stimulus of D2- and D3-preferring agonists in rats. Psychopharmacology 203, 317–327. http://dx.doi.org/10.1007/s00213-008-1323-4.
Lee, F.J.S., Pei, L., Moszczynska, A., Vukusic, B., Fletcher, P.J., Liu, F., 2007. Dopamine transporter cell surface localization facilitated by a direct interaction with the dopamine D_2 receptor. EMBO J. 26, 2127–2136. http://dx.doi.org/10.1038/sj.emboj.7601656.
Maggio, R., Millan, M.J., 2010. Dopamine D_2–D_3 receptor heteromers: pharmacological properties and therapeutic significance. Curr. Opin. Pharmacol. 10, 100–107. http://dx.doi.org/10.1016/j.coph.2009.10.001.
Millan, J.M., 2010. From the cell to the clinic: a comparative review of the partial D_2/D_3 receptor agonist and α2-adrenoceptor antagonist, piribedil, in the treatment of Parkinson's disease. Pharmacol. Ther. 128, 229–273. http://dx.doi.org/10.1016/j.pharmthera.2010.06.002.
Mason, C.W., Hassan, H.E., Kim, K.P., Cao, J., Eddington, N.D., Newman, A.H., Voulalas, P.J., 2010. Characterization of the transport, metabolism, and pharmacokinetics of the dopamine D3 receptor-selective fluorenyl- and 2-pyridylphenyl amides developed for treatment of psychostimulant abuse. J. Pharmacol. Exp. Ther. 333, 854–864. http://dx.doi.org/10.1124/jpet.109.165084.
Millan, M.J., Girardon, S., Monneyron, S., Dekeyne, A., 2000. Discriminative stimulus properties of the dopamine D3 receptor agonists, PD128,907 and 7-OH-DPAT: a comparative characterization with novel ligands at D3 and D2 receptors. Neuropharmacology 39, 586–598. http://dx.doi.org/10.1016/S0028-3908(99)00180-X.
Min, C., Zheng, M., Zhang, X., Caron, M.G., Kim, K.M., 2013. Novel roles of β-arrestins in the regulation of pharmacological sequestration to predict agonist-induced desensitization of dopamine D3 receptors. Br. J. Pharmacol. 170, 1112–1129. http://dx.doi.org/10.1111/bph.12357.
Miranda, M., Sorkin, A., 2007. Regulation of receptors and transporters by ubiquitination: new insights into surprisingly similar mechanisms. Mol. Interv. 7, 157–167. http://dx.doi.org/10.1124/mi.7.3.7.
Mortensen, O.V., Amara, S.G., 2003. Dynamic regulation of the dopamine transporter. Eur. J. Pharmacol. 479, 159–170. http://dx.doi.org/10.1016/j.ejphar.2003.08.066.
Neumaier, J.F., Root, D.C., Hamblin, M.W., 1996. Chronic fluoxetine reduces serotonin transporter mRNA and 5-HT1B mRNA in a sequential manner in the rat dorsal raphe nucleus. Neuropsychopharmacology 15, 515–522. http://dx.doi.org/10.1016/S0893-133X(96)00095-4.
Parkinson Study Group CALM cohort investigators, 2009. Long-term effect of initiating pramipexole vs levodopa in early Parkinson disease. Arch. Neurol. 66, 563–570. http://dx.doi.org/10.1001/archneur.66.1.nct90001.
Piercey, M.F., Hoffmann, W.E., Smith, M.W., Hyslop, D.K., 1996. Inhibition of dopamine neuron firing by pramipexole, a dopamine D3 receptor-preferring agonist: comparison to other dopamine receptor agonists. Eur. J. Pharmacol. 312, 35–44. http://dx.doi.org/10.1016/0014-2999(96)00454-2.
Platania, C.M., Salomone, S., Leggio, G.M., Drago, F., Bucolo, C., 2012. Homology modeling of dopamine D_2 and D_3 receptors: molecular dynamics refinement and docking evaluation. PLoS One 7, e44316. http://dx.doi.org/10.1371/journal.pone.0044316.
Salvatore, M.F., Apparsundaram, S., Gerhardt, G.A., 2003. Decreased plasma membrane expression of striatal dopamine transporter in aging. Neurobiol. Aging 24, 1147–1154. http://dx.doi.org/10.1016/S0197-4580(03)00129-5.
Schmid, J.A., Just, H., Sitte, H.H., 2001. Impact of oligomerization on the function of the human serotonin transporter. Biochem. Soc. Trans. 29, 732–736. http://dx.doi.org/10.1042/BST0290732.
Söderberg, O., Leuchowius, K.J., Gullberg, M., Jarvius, M., Weibrecht, I., Larsson, L.G., Landegren, U., 2008. Characterizing proteins and their interactions in cells and tissues using the in situ proximity ligation assay. Methods 45, 227–232. http://dx.doi.org/10.1016/j.ymeth.2008.06.014.
Sokoloff, P., Diaz, J., Le Foll, B., Guillin, O., Leriche, L., Bezard, E., Gross, C., 2006. The dopamine D3 receptor: a therapeutic target for the treatment of neuropsychiatric disorders. CNS Neurol. Disord. CNS Neurol. Disord. Drug Targets 5, 25–43. http://dx.doi.org/10.2174/187152706784111551.
Sokoloff, P., Giros, B., Martres, M.P., Bouthenet, M.L., Schwartz, J.C., 1990. Molecular cloning and characterization of a novel dopamine receptor (D3) as a target for neuroleptics. Nature 347, 146–151. http://dx.doi.org/10.1038/347146a0.
Torres, G.E., 2006. The dopamine transporter proteome. J. Neurochem. 97 (Suppl. 1), 3–10. http://dx.doi.org/10.1111/j.1471-4159.2006.03719.x.
Wang, Q., Mach, R.H., Luedtke, R.R., Reichert, D.E., 2010. Subtype selectivity of dopamine receptor ligands: insights from the structure and ligand-based methods. J. Chem. Inf. Model. 50, 1970–1985. http://dx.doi.org/10.1021/ci1002747.
Wersinger, C., Sidhu, A., 2003. Attenuation of dopamine transporter activity by alpha-synuclein. Neurosci. Lett. 340, 124–128. http://dx.doi.org/10.1016/S0304-3940(03)00097-1.
Zahniser, N.R., Sorkin, A., 2009. Trafficking of dopamine transporter in psychostimulant actions. Sem. Cell. Dev. Biol. 20, 411–417. http://dx.doi.org/10.1016/j.semcdb.2009.01.004.
Zapata, A., Kivell, B., Han, Y., Javitch, J.A., Bolan, E.A., Kuraguntla, D., Jaligam, V., Oz, M., Jayanthi, L.D., Samuvel, D.J., Ramamoorthy, S., Shippenberg, T.S., 2007. Regulation of dopamine transporter function and cell surface expression by D3 dopamine receptors. J. Biol. Chem. 282, 35842–35854. http://dx.doi.org/10.1074/jbc.M611758200.
Zapata, A., Shippenberg, T., 2002. D_3 receptor ligands modulate extracellular dopamine clearance in the nucleus accumbens. J. Neurochem. 81, 1035–1042. http://dx.doi.org/10.1046/j.1471-4159.2002.00893.x.
Zapata, A., Shippenberg, T., 2005. Lack of functional D2 receptors prevents the effects of D3-preferring agonist (+)-PD 128907 on dialysate dopamine levels. Neuropharmacology 48, 43–50. http://dx.doi.org/10.1016/j.neuropharm.2004.09.003.